Effect of impermeable barrier orientation on bottom water cresting

Hector Ngozi Akangbou[1]*, Martin Burby[2], Ghasem Nasr[3], Meisam Babaie[4]

[1234]Petroleum Technology and Spray Research Groups, School of Computing Science and Engineering, University of Salford, Manchester, United Kingdom, M5 4WT.

Abstract

The use of either a permeable or semi-permeable barriers has been proven to be effective in minimizing cresting effects in oil reservoirs characterized by strong bottom aquifer, with the latter known to be more effective. Most research has been focused on coning control in vertical wells with little research existing for cresting control in horizontal wells, especially in use of barriers.

Therefore, this paper sets out to numerically investigate the effect of an impermeable barrier orientation in an oil reservoir characterized by a strong bottom aquifer. The orientations considered in this study were horizontal and inclined (step-like) in terms of placement in the oil reservoir, modeled with similar thickness and width.

From the results, it was observed that a horizontally-placed impermeable barrier is more effective than inclined impermeable barriers in bottom water cresting scenarios. A horizontal impermeable barrier closer to the perforation of the horizontal well, 0.08*x* in thickness to the reservoir height and 0.45*x* to reservoir width was the most effective, although the effect of impermeable barrier width was found to be inconsistent with the performance of impermeable barriers. The study shows that the closer the entire top surface of the inclined impermeable barrier, the more effective the inclined impermeable barrier in minimizing bottom water cresting effect. The value of Reynolds number was found to be dependent on the orientation, thickness, position, and width of an impermeable barrier.

Keywords: Water cresting, Optimization, impermeable barrier.

1 Introduction

For over a decade, cresting in horizontal wells or coning in vertical wells has been a major problem in oil reservoirs characterized by strong gas cap and or strong bottom aquifer. Cresting in horizontal wells is often described as the protruded, crest-like movement of effluent(s) (unwanted water and or gas) in an oil reservoir towards the perforation of the horizontal well as a result of the imbalance of gravitational and viscous forces [1-4]. This results in displacement of oil by the effluent(s) towards the perforations of the well [1], until a breakthrough is experienced. At post-breakthrough, the effluent(s) dominate production, posing adverse effects in terms of overall oil productivity, operating and handling the cost of the water and/or gas produced and possibly the early shutting-in of wells [1]. Although cresting and coning are governed by similar principle, its effect in Horizontal wells is less detrimental due to the massive exposure of its laterals in the reservoir compared to vertical wells, resulting in a lower pressure drop and hence a preferred candidate in cresting scenarios [1].

For more than a decade, researchers have focused on coning/cresting control and prevention methods [5-33], gravity segregation [34, 35] and ICDs [36, 37]. Despite the wide research focus on coning control and prevention in vertical wells, little research exists for cresting control in horizontal wells [38]. Akangbou et al. [39] presented a novel experimental procedure to proactively control cresting in horizontal wells using an electromagnetic valve and effluent(s) breakthrough time. Yue et al. [28] numerically studied the effect of position and size of an impermeable barrier on bottom water cresting. They concluded that increase in impermeable barrier size (width and thickness) and vertical-displacement from the Water-Oil-Contact (WOC), yielded a higher critical rate. Yue et al. [38] investigated the effects of well, reservoir parameters, horizontally-placed semi-permeable and impermeable barriers on bottom water cresting. Yue et al. [27] numerically studied the effect of position and size of an assumed horizontal-placed, semi-permeable and impermeable barriers on bottom water cresting. They noticed that increase in semi-permeable barrier size, thickness and vertical position of the barrier resulted in a higher critical rate, hence a delay in bottom water breakthrough time. Although they stated that impermeable and semi permeable barriers can prevent or delay bottom water encroachment, they observed that the impermeable barrier performed better than the semi- permeable barrier but neglecting the effect its orientation in the reservoir for optimization purposes. Therefore, this paper sets out to numerically investigate the effect of impermeable barrier orientation, its vertical position, width and thickness in a homogeneous reservoir faced with bottom water cresting problem.

2 Reservoir and horizontal well models

The reservoir model and reservoir phases used in this investigation are illustrated in Figure 1. The reservoir model was assumed to be rectangular, homogeneous and consisted of 35 grid-blocks in the x-direction, 20 grid-blocks in the y-direction and 12 grid-blocks/layers in the z-direction with a total of 8400 active cells. Each grid block from layers 1-11 measured 40 ft in the x-direction, 60 ft in the y-direction and 5 ft in the z-direction while each grid block in layer 12 measured 40 ft in the x-direction, 60 ft in the y-direction and 10 ft in the z-direction. The reservoir fluids consist of water and oil phases. For sensitivity analysis, the adequate Fetkovich aquifer was connected to the entire base of water cell on Layer 12, to simulate the constant pressure of bottom water. The reservoir data and fluid properties are summarized in Table 1 while the data for Fetkovich aquifer is illustrated in Table 2. The initial aquifer pressure for the Fetkovich aquifer was defaulted, thereby placing the aquifer as close as possible to equilibrium with the reservoir pressure.

The horizontal well and its lateral placement in the in the reservoir is illustrated in Figure 2. As shown in Figure 2, the horizontal well model was located at i = 4-35 (opened to liquid production from i = 6-35), j = 11 and k = 2, far away from the WOC or layer saturated with water (Layer 12) due to the presence of strong bottom aquifer.

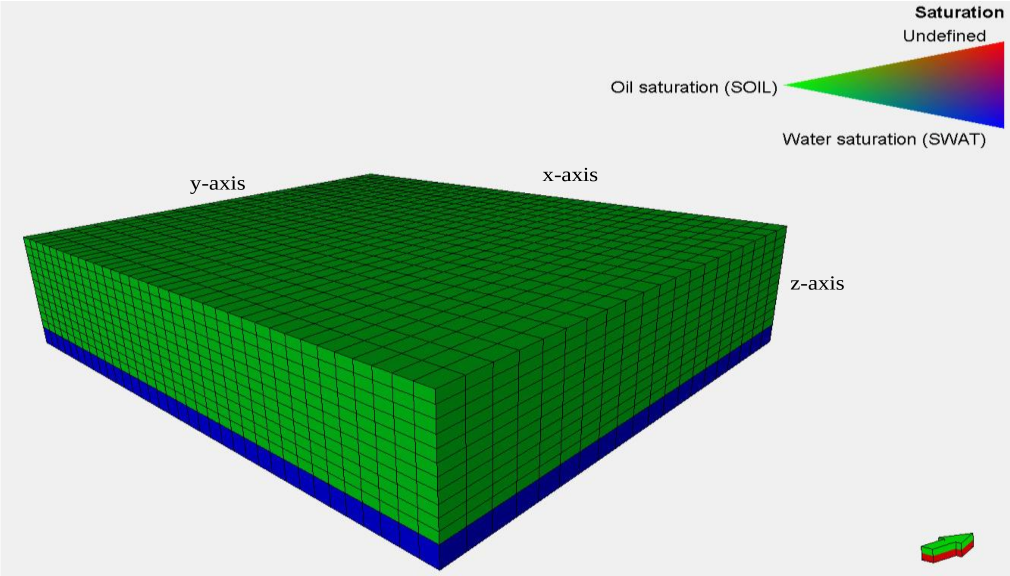

Figure. 1. Reservoir model showing oil and water saturations.

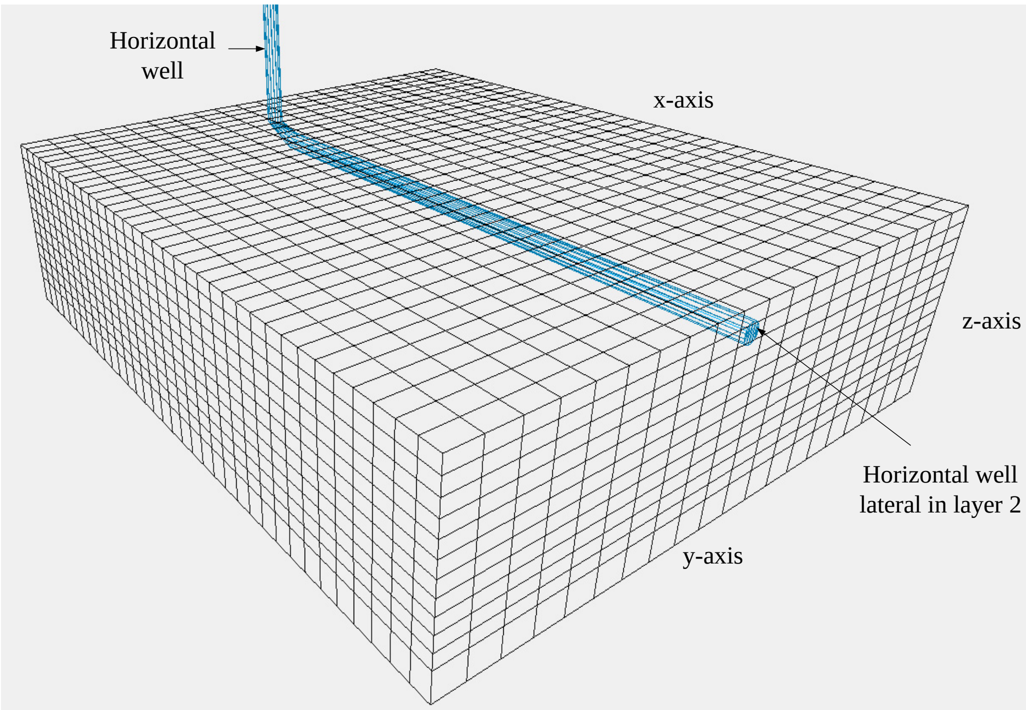

Figure. 2. Horizontal well in reservoir.

Table 1. Reservoir and horizontal well data

Parameter	Value
Reservoir thickness (ft)	65
Reservoir length (ft)	1400
Reservoir width (ft)	1200
Reservoir Pressure (psia)	2500
Horizontal well Datum depth (ft)	6164
Permeability in x, y and z directions (mD)	7000

Horizontal well production rate (stb/day)	9000
Reservoir Water Compressibility (1/psi)	$3.0e^{-6}$
Reservoir oil Density (ρ_o), lb/ft^3	58
Reservoir water Density (ρ_w), lb/ft^3	64.2
Reservoir water Viscosity (μ_w), cP	0.48
Reservoir oil Compressibility (1/psi)	$1.5e^{-5}$
Reservoir oil viscosity (μ_o), cP	3.8
Porosity (oil zone)	0.35
Porosity (water zone)	$1e^{10}$
Horizontal well diameter (ft)	0.41667

Table 2. Data for Fetkovich aquifer

Parameter	Fetkovich aquifer
Datum depth (ft)	6209
Aquifer Productivity Index (stb/day/psi)	5
Thickness of aquifer (ft)	10
Lower *i* connection	1
Upper *i* connection	35
Lower *j* connection	1
Upper *j* connection	20
Lower *k* connection	1
Upper *k* connection	12
Face	*K+*
Initial volume of water in aquifer (ft^3)	$1.0e^{-5}$
Total compressibility of the aquifer (1/psi)	$1.0e^{-5}$

3 Impermeable barriers

A conceptual design of the different orientation of impermeable barriers used in this investigation on the x-z axis and y-z axis are illustrated in Figure 3. The impermeable barrier effective permeability was modeled by setting the effective permeability for the region of interest or grid blocks to zero (0 mD). In Figure 3, a_1 and a_2 represent the distance of horizontal well to inclined (step-like) impermeable barrier, c represents the distance of horizontal well to horizontal impermeable barrier, h_w represents the height/thickness of the aquifer, h_o represents the height of the oil/pay zone, h_t represents the height/thickness of the reservoir, b_1 and b_2 represents the distance of inclined impermeable barrier to the WOC, d represents the distance of horizontal impermeable barrier to the WOC, w represents the width of the impermeable barriers while e and f represents the thickness of the inclined and horizontal impermeable barriers respectively. The values of nomenclature used to describe the impermeable barriers in Figure 3 are summarized in Table 3. For close comparison between the horizontal and inclined impermeable barriers, the same number of impermeable reservoir grid blocks in the x-z and y-z axes were simulated for each case. A detailed summary of all simulation cases used in this investigation for horizontal and inclined barriers are shown in Tables 4 and 5 respectively. For this investigation, it was assumed that the modeling of the Impermeable barrier has no effect on the Overall Oil in Place.

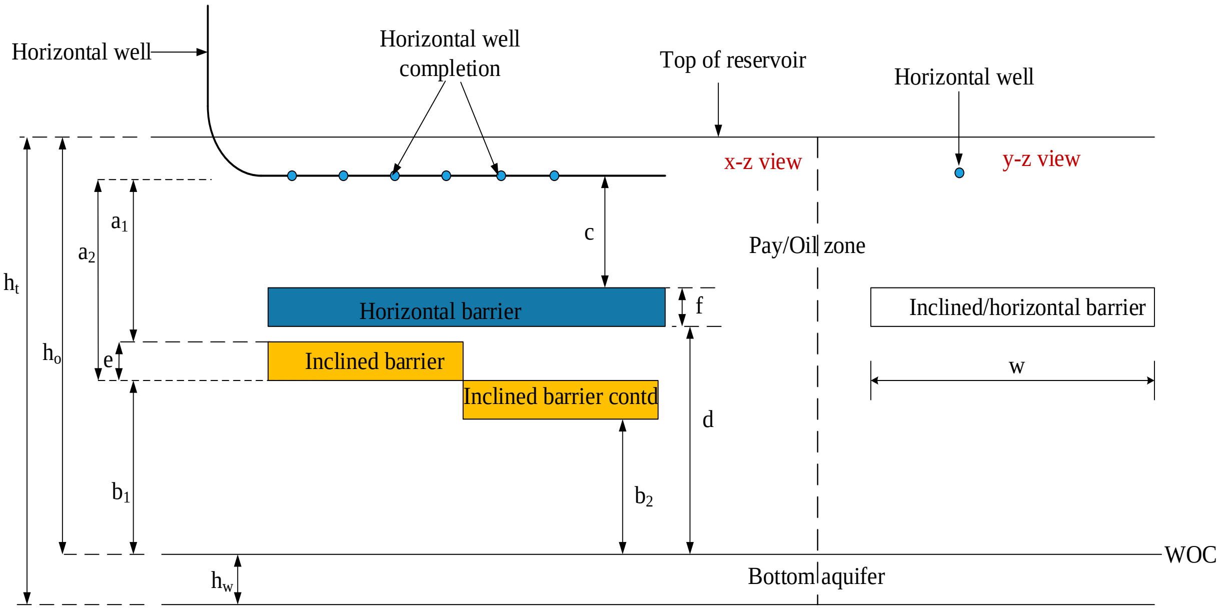

Figure. 3. Orientations of impermeable barriers on the x-z axis and y-z axis in the reservoir.

Table 3. Input data for Impermeable barrier sensitivity simulations

Parameter	Horizontal barrier(s)	Inclined barrier(s)
Thickness of barrier (ft)	*f* = 5, 10, 15	*e* = 5, 10, 15
Width of barrier (ft)	*w* = 420, 540, 660	*w* = 420, 540, 660
Length of barrier (ft)	1200 (grid block 6-35)	1200 (grid block 6-35)
Distance of horizontal well to impermeable barrier (ft)	*c* = 10, 15	a_1 = 10, 15;
		a_2 = 15, 20, 25, 30
Distance of impermeable barrier to WOC (ft)	*d* = 15, 20, 25, 30	b_1 = 15, 20, 25, 30;
		b_2 = 0, 5, 10, 15, 20, 25

Table 4. Detailed description of cases used for horizontal impermeable barrier simulations

Cases	*f* (ft)	*c* (ft)	*w* (ft)	*d* (ft)
Case 1	-	-	-	-
Case 2	5	10	420	30
Case 3	5	10	540	30
Case 4	5	10	660	30
Case 5	5	15	420	25
Case 6	5	15	540	25
Case 7	5	15	660	25
Case 2A	10	10	420	25
Case 3A	10	10	540	25
Case 4A	10	10	660	25
Case 5A	10	15	420	20
Case 6A	10	15	540	20
Case 7A	10	15	660	20
Case 2B	15	10	420	20
Case 3B	15	10	540	20

Case 4B	15	10	660	20
Case 5B	15	15	420	15
Case 6B	15	15	540	15
Case 7B	15	15	660	15

Table 5. Detailed description of cases used for inclined (step-like) impermeable barrier simulations

Cases	*e* (ft)	a_1 (ft)	a_2 (ft)	*w* (ft)	d_1 (ft)	d_2 (ft)
Case 1	-	-	-	-	-	-
Case 2C	5	10	15	420	30	25
Case 3C	5	10	15	540	30	25
Case 4C	5	10	15	660	30	25
Case 5C	5	15	20	420	25	20
Case 6C	5	15	20	540	25	20
Case 7C	5	15	20	660	25	20
Case 2D	10	10	20	420	25	15
Case 3D	10	10	20	540	25	15
Case 4D	10	10	20	660	25	15
Case 5D	10	15	25	420	20	10
Case 6D	10	15	25	540	20	10
Case 7D	10	15	25	660	20	10
Case 2E	15	10	25	420	20	5
Case 3E	15	10	25	540	20	5
Case 4E	15	10	25	660	20	5
Case 5E	15	15	30	420	15	0
Case 6E	15	15	30	540	15	0
Case 7E	15	15	30	660	15	0

4 Results and discussion

Sets of simulation cases defined in Tables 4 and 5 were used to carry out sensitivity analyses in an oil reservoir affected by bottom water cresting problem. The simulation for each case was run from May-2017 to December-2023. From Table 3 in *section 3,* the total number of impermeable barrier grid block(s) simulated ranged between 0-990.

Figure 4 illustrates the permeability results of simulated impermeable barriers for different cases. Figure 4(a) represents the permeability results on the y-z axis for case 7B while Figure 4(b) represents the permeability result for Case 2A on the y-z axis. Figure 5 depicts the simulation result of water cresting occurring in a formation with no defined impermeable barrier (Case 1/base case) on the y-z axis. Figure 5(a) shows the reservoir at static condition (Time, T = 0 days) while Figure 5(b-d) illustrates water cresting process at T = 300, 600 and 900 days respectively. Figure 6 shows the simulation result of water cresting occurring in a formation with a defined horizontal impermeable barrier for Case 2A (f = 10 ft, c = 10 ft, w = 420 ft and d = 25 ft) on the y-z axis. Figure 6(a) shows the reservoir at static condition (T = 0 days) while Figure 6(b-d) illustrates water cresting process at T = 300, 600 and 1500 days respectively. Figure 7 shows the simulation result of water cresting occurring in a formation with a defined horizontal impermeable barrier for Case 7B (f = 15 ft, c = 15 ft, w = 660 ft and d = 15 ft) on the y-z axis. Figure 7(a) shows the reservoir at static condition (T = 0 s) while Figure 7(b-c) illustrates water cresting process at T = 300, 600 and 1500 days respectively.

From the simulation results presented in Figures 5-7, it can be clearly seen that an impermeable barrier impedes the rise of bottom water during cresting and distorts the crest-like shape. More so, the bottom water height can be seen to be closer to the horizontal well in Case 1 compared to Cases 2A and 7B at about 300 days, reaching the perforations of the horizontal well in layer 2 at about 600 days.

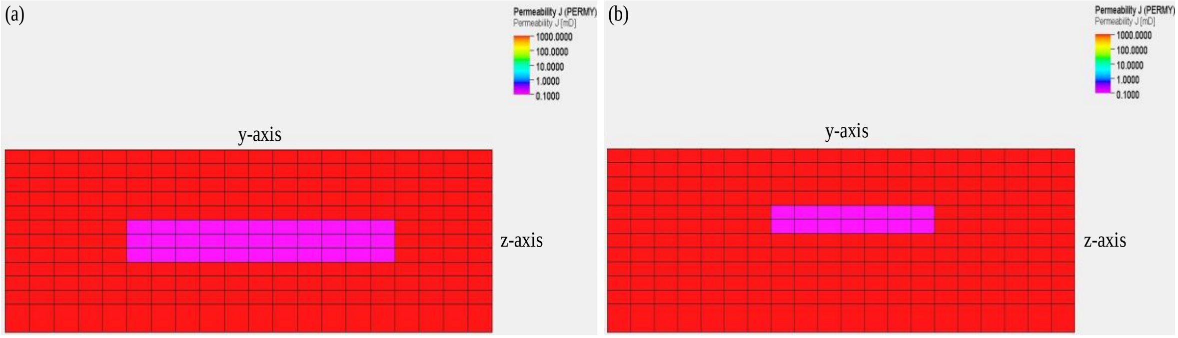

Figure. 4. Formation with impermeable barriers (a) Case 7B, (b) Case 2A.

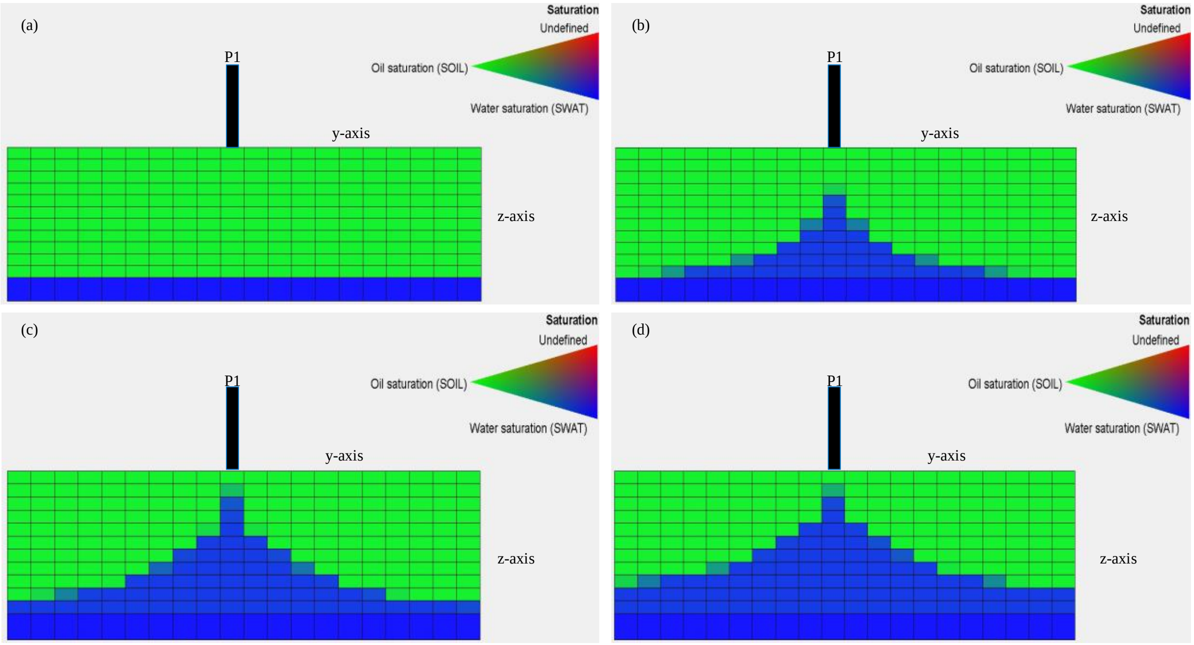

Figure. 5. Water cresting process for Case 1 at (a) static condition (T = 0 day), (b) simulation at T= 300 days, (c) simulation at T = 600 days, (d) simulation at T = 900 days.

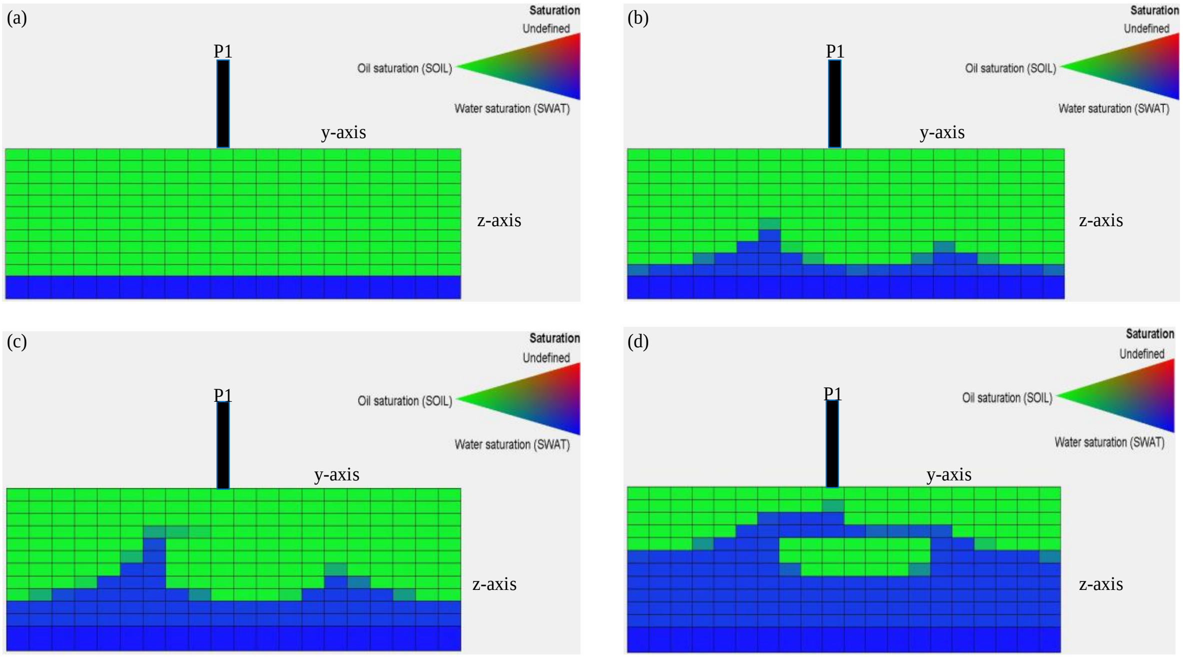

Figure. 6. Water cresting process for Case 2A at (a) static condition (T = 0 day), (b) simulation at T = 300 days, (c) simulation at T = 600 days, (d) simulation at T = 1500 days.

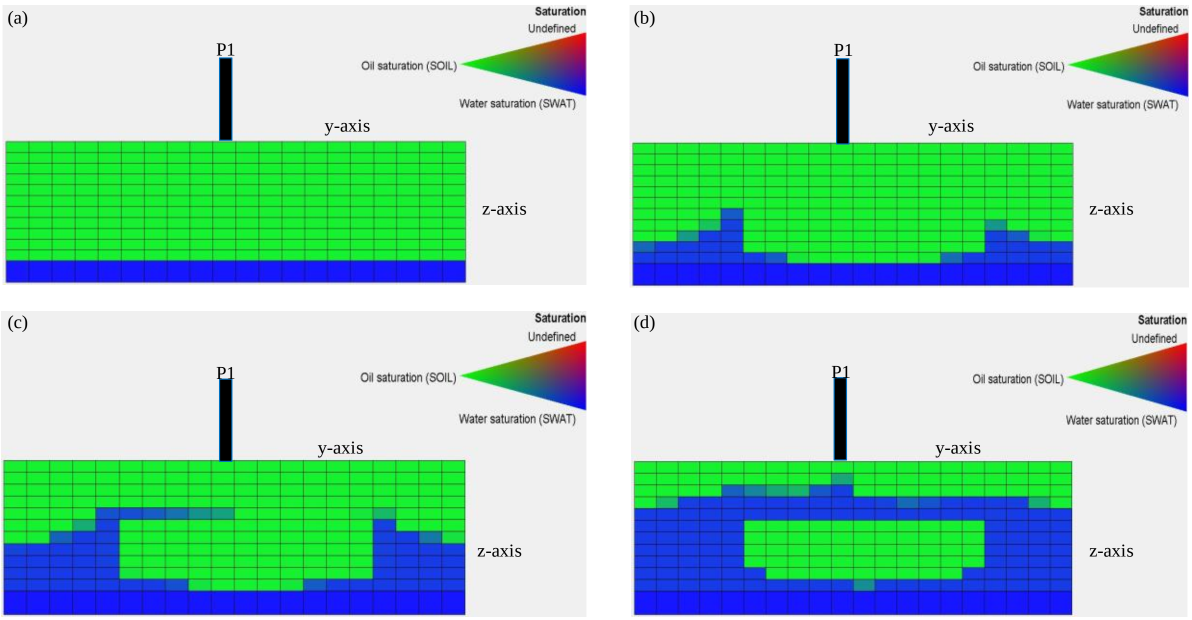

Figure. 7. Water cresting process for Case 7B at (a) static condition (T = 0 day), (b) simulation at T = 300 days, (c) simulation at T = 600 days, (d) simulation at T = 1500 days.

4.1 Effect of impermeable barrier thickness on oil and water production cumulative

Figures 8 and 9 illustrate the effect of impermeable barrier thickness on oil and water production cumulative for horizontal and inclined impermeable barriers respectively, in standard cubic meters (sm^3). In Figure 8, Cases 1, 2, 2A, 2B, 3, 3A, 3B were simulated to determine the effect of horizontal impermeable barrier thickness on oil and water production cumulative. To determine this effect, Tables 4 and 5 in *section 3* were considered. Hence, Cases 2, 2A, 2B (*scenario 1*) and Cases 3, 3A, 3B (*scenario 2*) were compared separately.

As expected, Figure 8 shows that Case 1 had the lowest oil production cumulative and highest water production cumulative when compared with all cases. More so, it was observed that the thicker the impermeable barrier, the lower the oil production cumulative and the higher the water production cumulative, contradicting the results presented by Yue et al. [28]. In *scenario 1*, highest oil production cumulative was observed in Case 2 (383956.62 sm^3) and least in Case 2B (358798.31 sm^3) while the highest water production cumulative was observed in Case 2B (343699.63 sm^3) and least in Case 2 (315334.53 sm^3). In scenario 2, highest oil production cumulative was observed in Case 3 (384677.22 sm^3) and least in Case 3B (355229.97 sm^3) while the highest water production cumulative was observed in Case 3B (347722.78 sm^3) and least in Case 3 (314521.72 sm^3).

In Figure 9, Cases 1, 2C, 2D, 2E, 5C, 5D, 5E were simulated to determine the effect of inclined impermeable barrier thickness on oil and water production cumulative. *Scenario 3* (Cases 2C, 2D and 2E) and *Scenario 4* (Cases 5C, 5D and 5E). A similar trend to Figure 8 was observed in Figure 9. In *scenario 3 and 4*, highest oil production cumulative was observed in Cases 2C and 5C respectively while highest water production cumulative was observed in Cases 2E and 5E respectively.

We believe that an impermeable barrier not only minimizes water cresting effect but also negatively affects the mobility of the reservoir oil around the impermeable barrier. Therefore, the thinner the barrier thickness, the better the performance of horizontal wells in reservoirs with strong bottom water.

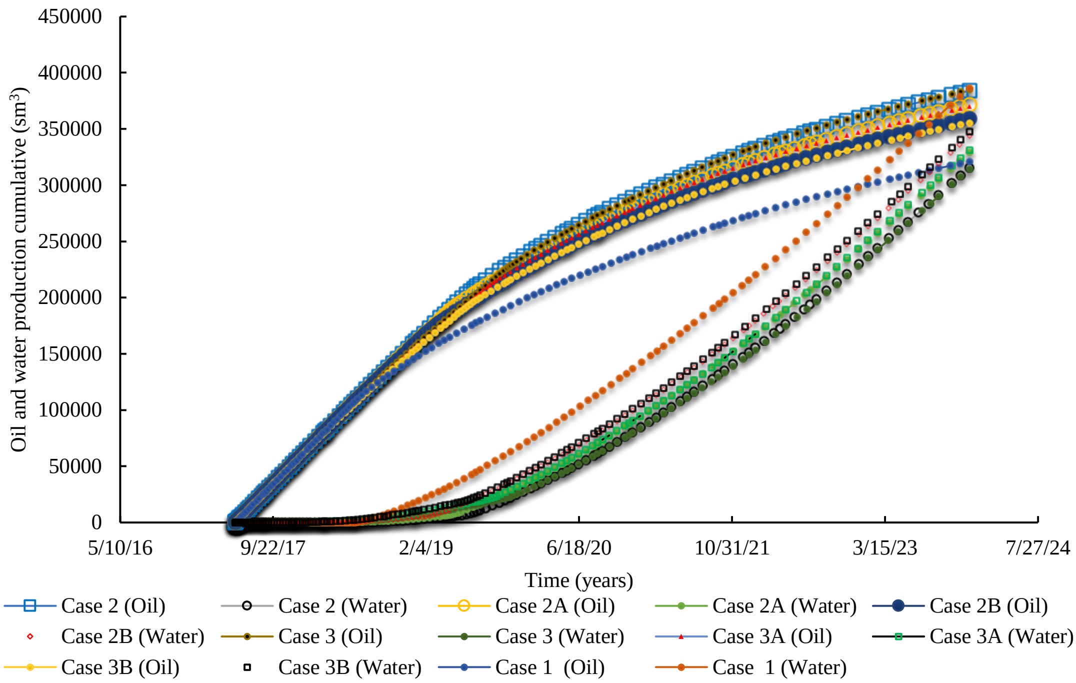

Figure. 8. Effect of horizontal impermeable barrier thickness on cumulative oil and water production cumulative.

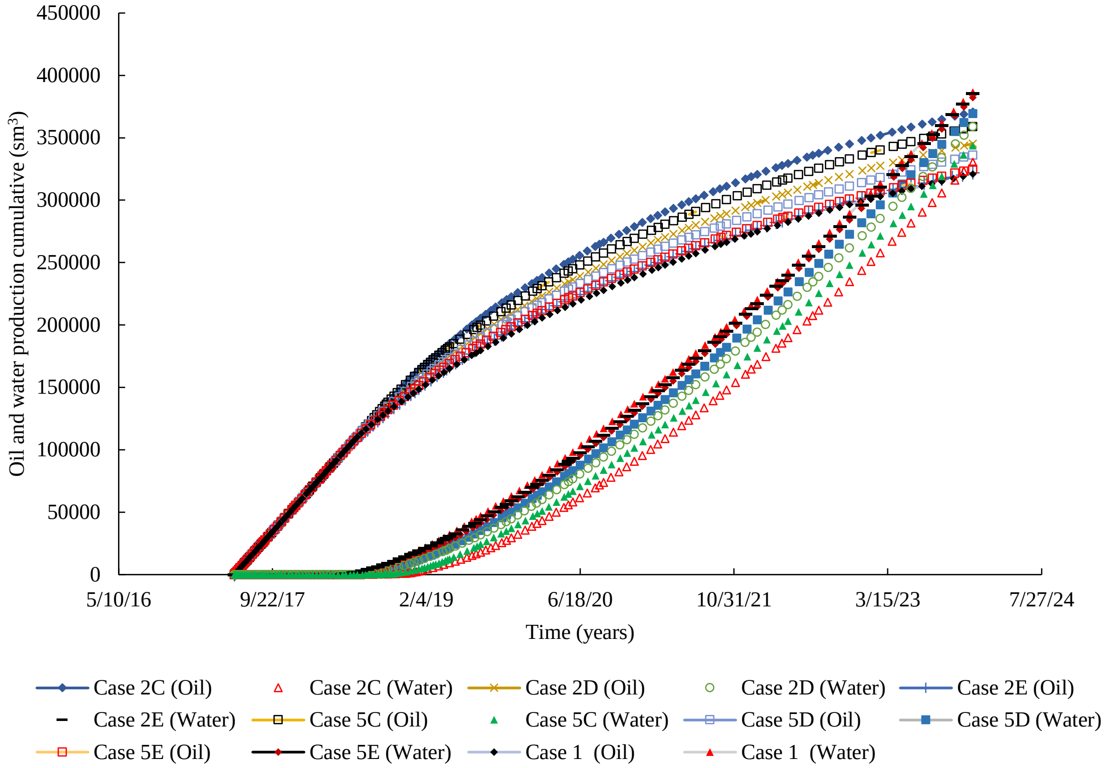

Figure. 9. Effect of inclined impermeable barrier thickness on oil and water production cumulative.

4.2 Effect of impermeable barrier width on oil and water production cumulative

Figures 10 and 11 illustrate the effect of impermeable barrier width on oil and water production cumulative for horizontal and inclined impermeable barriers respectively. In Figure 10, Cases 1, 2, 3, 4, 5B, 6B and 7B were simulated to determine the effect of horizontal impermeable barrier width on oil and water production cumulative. As expected, Case 1 had the lowest oil production cumulative (320821.41 sm^3) and highest water production cumulative (386515.56 sm^3) when compared with all cases. From Table 4 in *section 3*, Cases 2, 3, 4 and Cases 5B, 6B and 7B were compared separately in terms of oil and water production cumulative. As shown in Figure 10, Cases 3 (0.45*x* the reservoir width) and 5B had the highest oil production cumulative of 384677.22 sm^3 and 345857.25 sm^3 respectively while the highest water production cumulative was observed in Cases 4 (322828.44 sm^3) and 7B (372022.97 sm^3). This inconsistency in results is contrary to that reported by Yue et al. [27]. Therefore, an increase in impermeable barrier width does not always result in higher oil and lower water production cumulative. We believe the reason for this inconsistent trend is due to an optimum impermeable barrier condition which involves the vertical position of the impermeable barrier in the reservoir and thickness which could influence the mobility of the reservoir phases.

In Figure 11, Cases 2D, 3D, 4D, 5E, 6E, and 7E were simulated to determine the effect of inclined impermeable barrier width on oil and water production cumulative. In Figure 11, Cases 2D, 3D, 4D and Cases 5E, 6E, 7E were compared separately. Cases 2D and 5E had highest oil production cumulative and lowest water production cumulative when compared with the worst cases (4D and 7E). Hence for a reduction of barrier width by 36% (from 660 ft to 420 ft), an increment of 10579.03 sm^3 in oil production cumulative was `observed between Cases 2D and 4D while an increment of 4959.19 sm^3 in oil production cumulative was observed between Cases 5E and 7E. In addition, a decrement in water production cumulative (11927.62 sm^3) was observed between Cases 2D and 4D while a decrement of (5591.66 sm^3) was observed for oil production cumulative between Cases 5E and 7E.

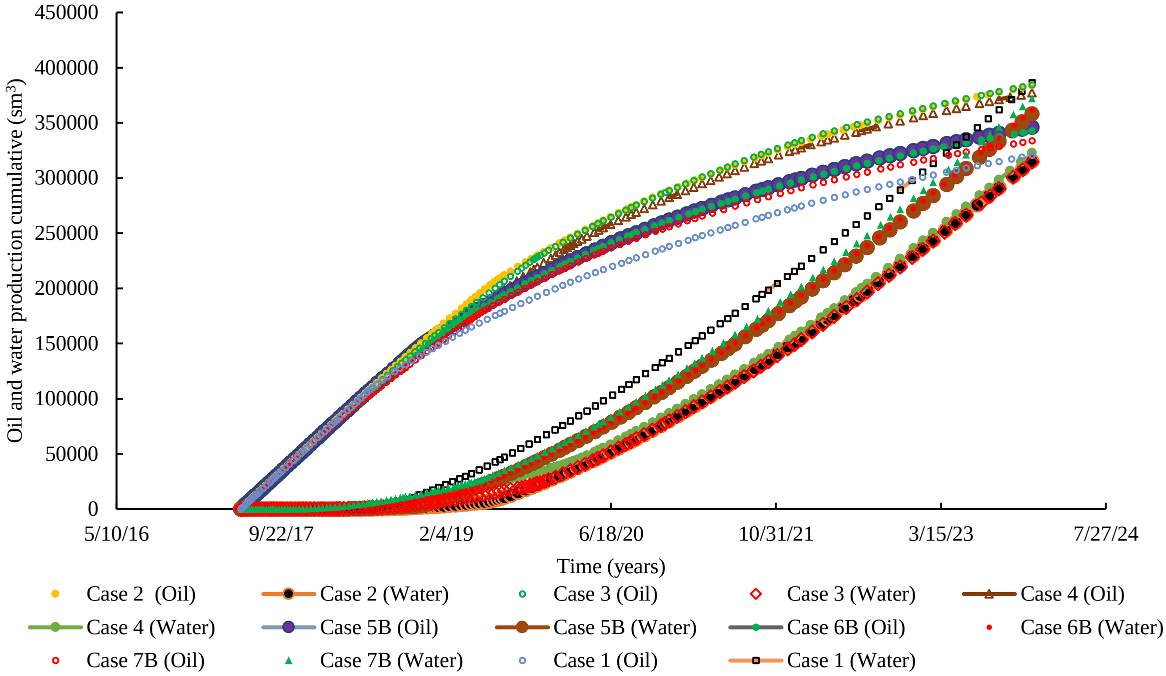

Figure. 10. Effect of inclined impermeable barrier width on oil and water production cumulative.

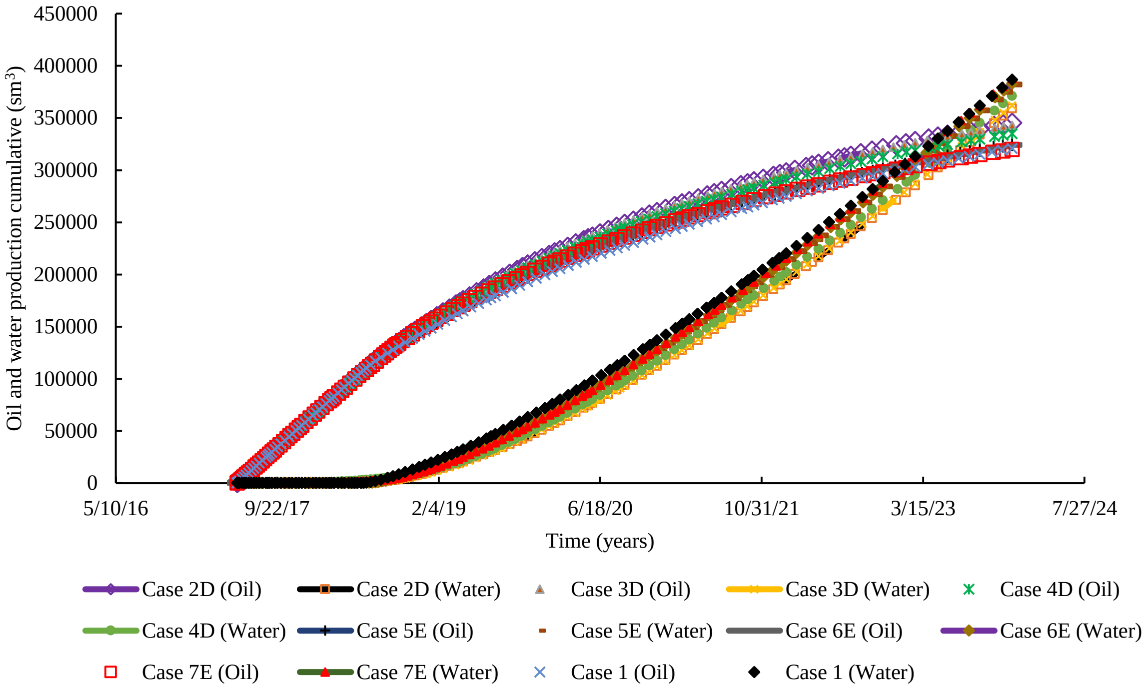

Figure. 11. Effect of inclined impermeable barrier width oil and water production cumulative.

4.3 Effect of impermeable barrier position (vertical) on oil and water production cumulative

The effect of impermeable barrier vertical position on oil and water production cumulative for horizontal and inclined impermeable barriers are shown in Figures 12 and 13 respectively. In Figure 12, Cases 2, 5 and Cases 3B and 6B were compared separately in terms of oil and water production cumulative. It was observed that Cases 2 and 3B had the higher oil production cumulative of 383956.62 sm^3 and 355229.97 sm^3 respectively at lower water production cumulative.

In Figure 13, Cases 1, 4C, 7C, 4D and 7D were simulated to determine the effect of inclined impermeable barrier vertical position on oil and water production cumulative. At the stop of simulation, Case 1 can be seen to achieve the lowest oil production cumulative and highest water production cumulative when compared with all cases. In Figure 13, Cases 4C, 7C, and Cases 4D, 7D were compared separately. Cases 4C and 5D can be seen to have higher oil production cumulative and lowest water production cumulative when compared with Cases 7C and 7D respectively. Therefore, an increase in depth of both inclined and horizontal impermeable barriers resulted in lower oil production cumulative and higher water production cumulative, which was in good agreement with Yue et al. [27],[28].

Figure 14 illustrates the effect of vertical displacement of the horizontal well to the inclined impermeable barrier ($a_1 \neq a_2$), simulated between Cases 7C, 7D, and 7E. As shown in Figure 14, the closer a_1 is to a_2, the more effective the impermeable barrier. Hence highest oil production cumulative (352608.41 sm^3) and lowest water production cumulative (350677.97 sm^3) was observed compared to Cases 7D and 7E. A similar trend can be seen to occur between Cases 5C, 5D, and 5E.

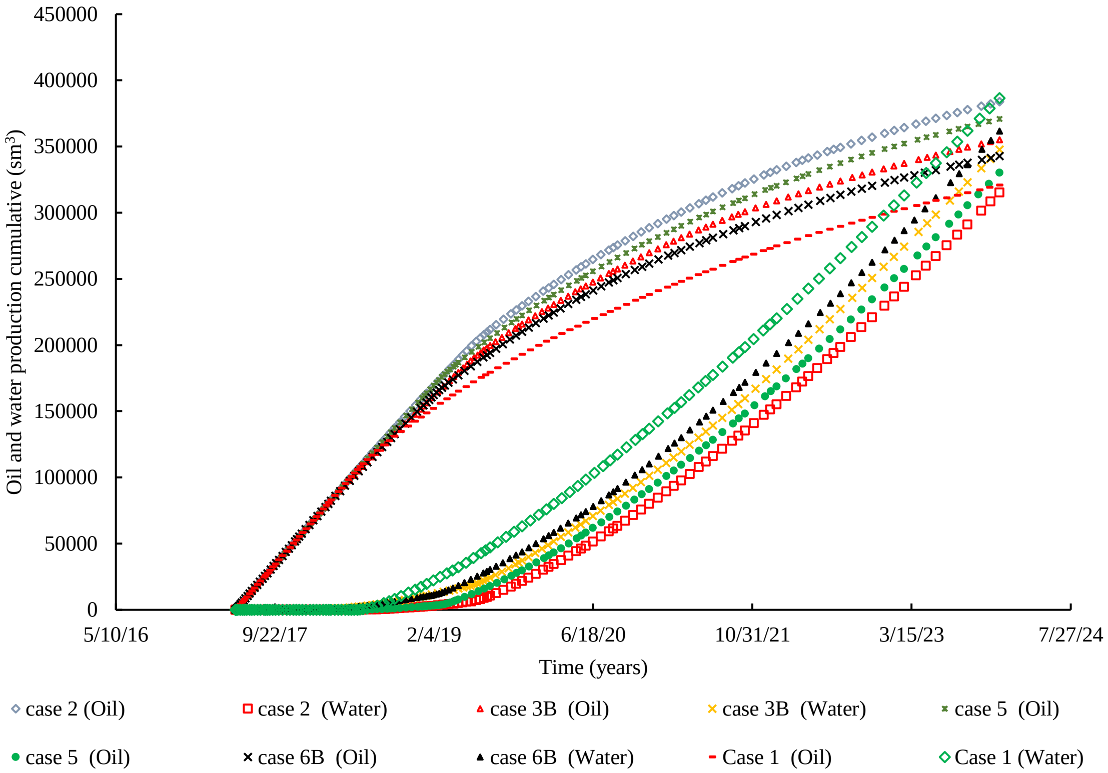

Figure. 12. Effect of inclined impermeable position width on oil and water production cumulative.

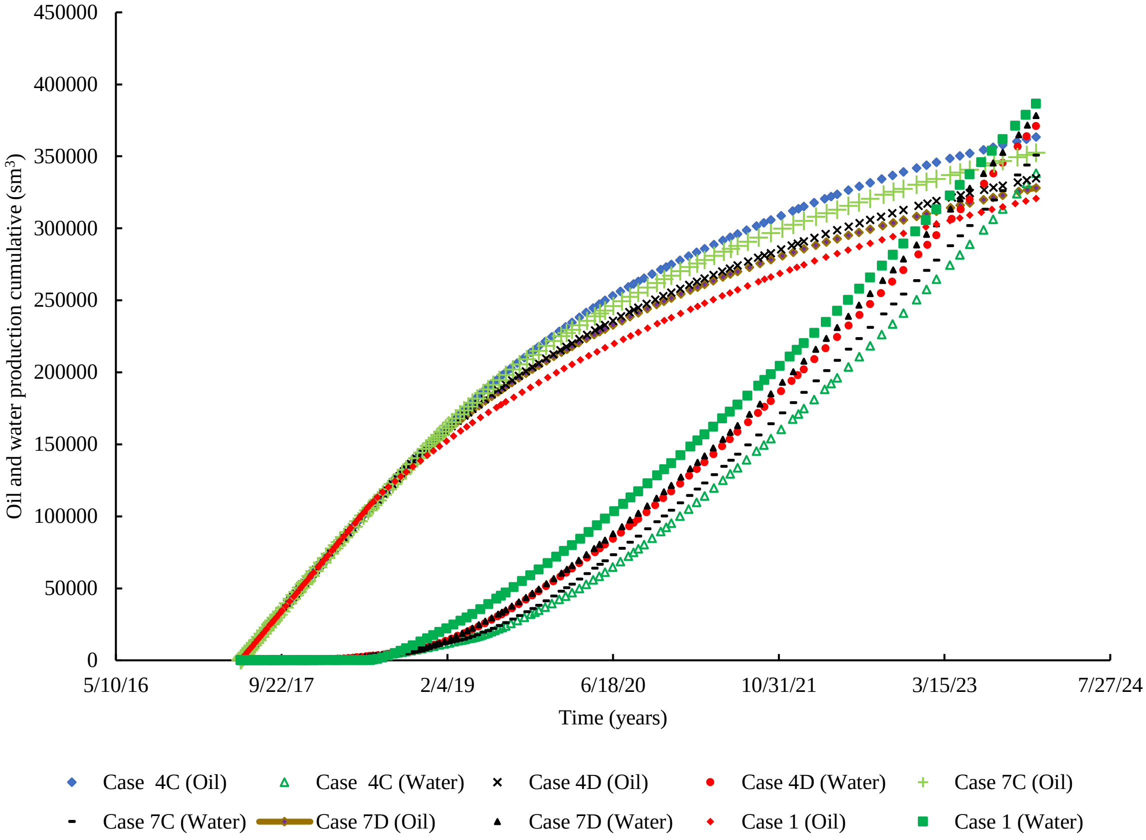

Figure. 13. Effect of inclined impermeable barrier position on oil and water production cumulative.

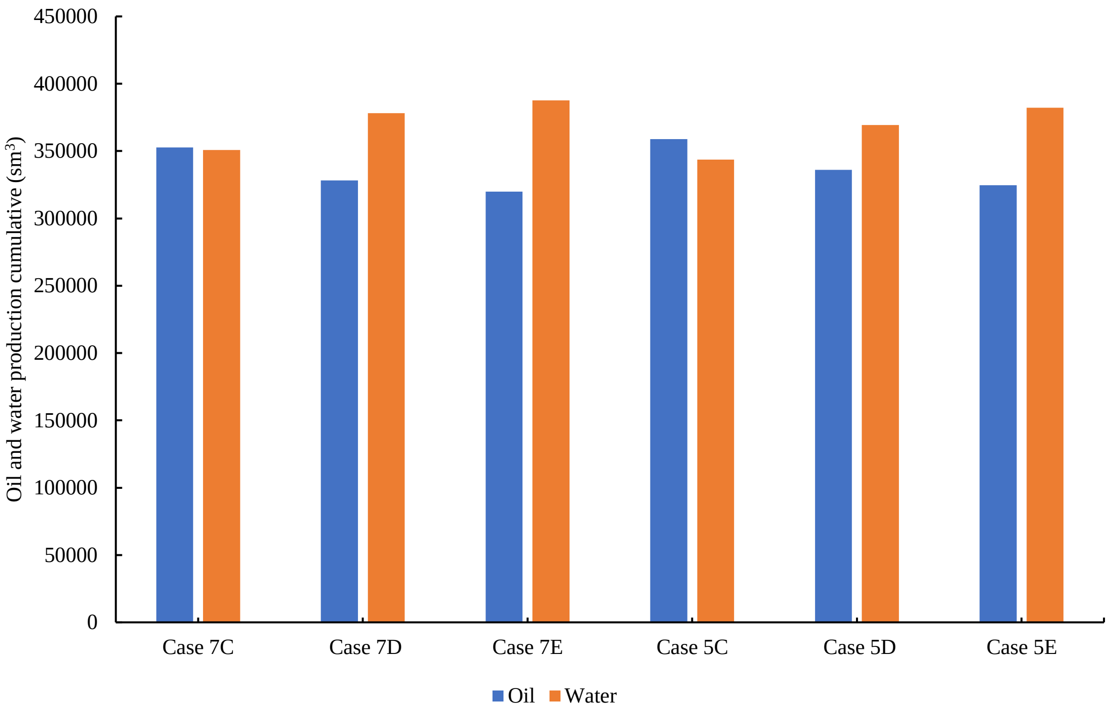

Figure. 14. Effect of the vertical displacement of horizontal well to inclined impermeable barrier oil and water production cumulative.

4.3 Comparison on the effects of inclined and horizontal barriers on oil and water production cumulative

Figure 15 illustrates a comparison between inclined and horizontal barriers in terms of oil and water production cumulative. The best cases (Cases 1, 3C, 3, 6, 2A, 5A, 2B, 5B, 6C, 2D, 5D, 2E and 5E) from the effects of impermeable barrier width, thickness, and vertical positions are represented and compared graphically in Figure 15. As shown in Figure 15, Case 1 is seen to have the highest water production cumulative as well as the least oil production cumulative while Case 3 (horizontal impermeable barrier) achieved the highest oil production cumulative (384677.22 sm^3) and least water production cumulative (314521.72 sm^3). Therefore, in all cases, an optimum horizontal impermeable barrier is recommended in reservoirs with strong bottom water.

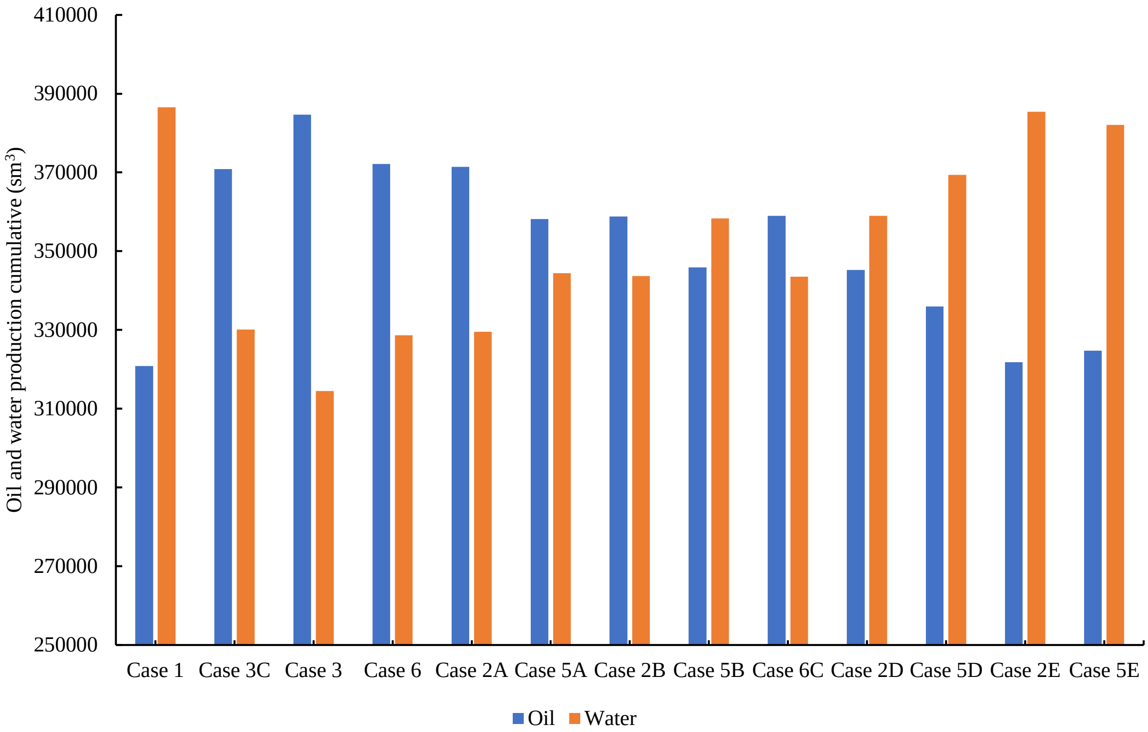

Figure. 15. Comparison of inclined and horizontal barriers.

4.4 Effect of impermeable barrier on Reynolds number

Figures 16 and 17 illustrate the effect of impermeable barrier on Reynolds number for horizontal and inclined impermeable barriers respectively. A similar equation (Equation 1) for estimation of Reynolds number (R_e) used by Akangbou et al. [1], was applied in this study. In Equation 1, the horizontal well diameter specified in Table 1 was assumed to be equal to the inside diameter of the horizontal well. Unlike Akangbou et al. [1], actual (not cumulative) oil flow rates were used and the estimated Reynolds number in Figures 16 and 17 were greater than 2000 ($R_e > 2000$), depicting a turbulent flow regime between July-2018 and July-2021. As shown in Figures 16 and 17, horizontal and inclined impermeable barriers affect the Reynolds number during cresting. Case 1 can be seen to have lower turbulence compared to Cases 2, 3, 4, 2C, 3C and 4C.

$$R_e = \frac{\rho_o D_i Q_o}{\mu_o A} \tag{1}$$

Where Q_o is the oil flow rate in cubic meter per second, D_i is the inside diameter of the horizontal well in meters, μ_o is the viscosity of the oil in Newton-second per square meter, ρ_o is the density of the oil in Kilogram per cubic meters, A is the cross-sectional area of the horizontal well in square meters and R_e is the Reynolds number in dimensionless unit.

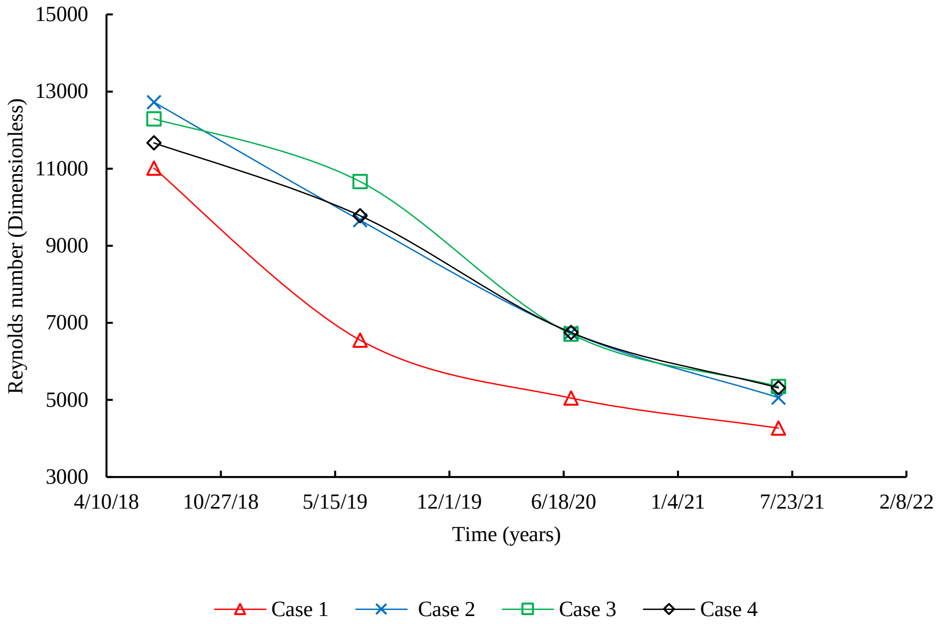

Figure. 16. Effect of impermeable barrier on Reynolds number (horizontal impermeable barrier cases).

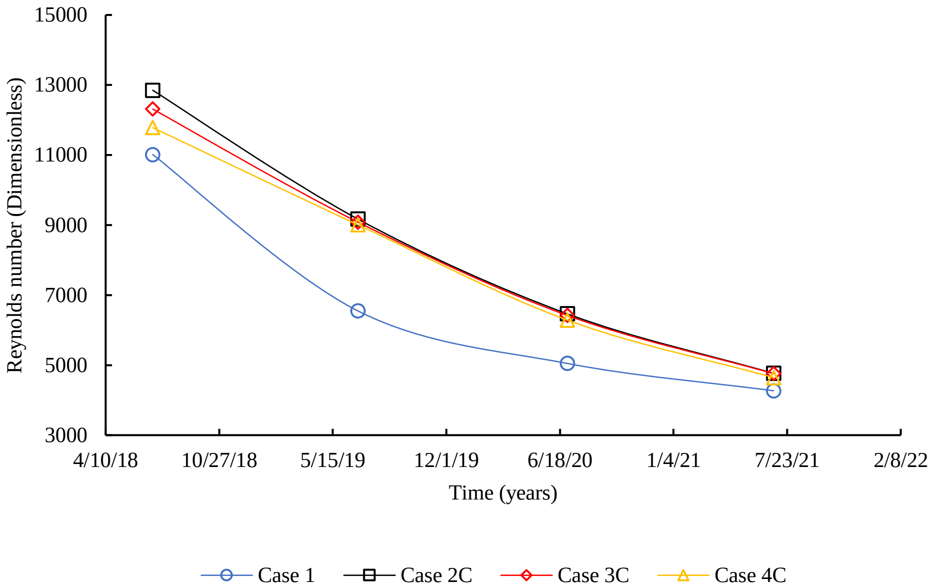

Figure. 17. Effect of impermeable barrier on Reynolds number (inclined impermeable barrier cases).

5 Conclusion

A rigorous numerical study was performed on the effects of the orientation of impermeable barriers on bottom water cresting. From the analyses, it can be concluded that:

1. The orientation of an impermeable barrier is important for minimizing bottom water cresting effect. An optimum horizontally-placed impermeable barrier was found to be more effective when compared with inclined impermeable barriers. For inclined impermeable barriers, the closer the height of a_1 and a_2, the more effective the impermeable barrier.
2. The effectiveness of an impermeable barrier is insensitive to its width. The thinner the impermeable barrier and the closer the top of the impermeable barrier to the horizontal well the more effective the impermeable barrier. A horizontal impermeable barrier; 0.08*x* in thickness to the reservoir height and 0.45*x* to reservoir width was found to be most effective.
3. The presence of an impermeable barrier results in an increase in Reynolds number. Water cresting is independent of Reynolds number and Reynolds number depends on the orientation, thickness, position, and width of an impermeable barrier during cresting.

References

1. Akangbou, H.N., Burby, M., and Nasr, G., "Effectively optimizing production of horizontal wells in homogeneous oil reservoirs", Journal of Petroleum Science and Engineering 2017; 150:128-136.

2. Kromah, M.J. and Dawe, R.A., "Reduction of Oil and Gas Coning Effects by Production Cycling and Horizontal Wells", Petroleum Science and Technology 2008; 26(3):353-367.

3. Makinde, F.A., Adefidipe, O.A., and Craig, A.J., "Water Coning in Horizontal Wells: Prediction of Post-Breakthrough Performance", International Journal of Engineering & Technology 2011; (11)1.

4. Permadi, P., "Fast Horizontal-Well Coning Evaluation Method", Society of Petroleum Engineers 1996.

5. Dai, L.C., et al., "Case Study on Polymer Gel to Control Water Coning for Horizontal Well in Offshore Oilfield", Offshore Technology Conference 2011.

6. Kantzas, A., et al., "Design Strategies For Improved Conformance Using Polymer Gels", Petroleum Society of Canada 1994.

7. Law, D.S. and Jossy, W.E., "Visualization Study of Anti-water Coning Process Using Gels", Petroleum Society of Canada 1996.

8. Thakur, G.C. and Tachuk, A.R, "Retardation Of Water Coning In Oil Wells Using Polymers - A Reservoir Simulation Application", Petroleum Society of Canada 1974.

9. White, J.L., Goddard, J.E, and Phillips, H.M., "Use of Polymers To Control Water Production in Oil Wells", Society of Petroleum Engineers 1973.

10. Zaitoun, A., Kohler, N., and Montemurro, M.A., "Control of Water Influx in Heavy-Oil Horizontal Wells by Polymer Treatment", Society of Petroleum Engineers 1992.

11. Albonico, P., et al., "New Polymer Gels for Reducing Water Production in High-Temperature Reservoirs", Society of Petroleum Engineers 1994.

12. Lakatos, I., et al., "Restriction of Gas Coning by a Novel Gel/ Foam Technique", Society of Petroleum Engineers 1998.

13. Surguchev, L.M., "Water Shut-Off: Simulation and Laboratory Evaluation", Society of Petroleum Engineers 1998.

14. Shirif, E., "Mobility Control by Polymers Under Bottom-Water Conditions, Experimental Approach", Society of Petroleum Engineers 2000.

15. Zaitoun, A. and Pichery, T., "A Successful Polymer Treatment For Water Coning Abatement in Gas Storage Reservoir", Society of Petroleum Engineers 2001.

16. Ghahfarokhi, R.B., Green, D.W., and Liang, J.T., "Simulation of Gelled Polymer Treatments in the Arbuckle Formation", Society of Petroleum Engineers 2006.

17. Vasquez, J.E., et al., "Organically Crosslinked Polymer System for Water Reduction Treatments in Mexico", Society of Petroleum Engineers 2006.

18. El-karsani, K.S.M., Al-Muntasheri, G.A., and Hussein, I.A., "Polymer Systems for Water Shutoff and Profile Modification: A Review Over the Last Decade", Society of Petroleum Engineers 2014.

19. Al-Muntasheri, G.A., et al., "Water Shut-off with Polymer Gels in A High Temperature Horizontal Gas Well: A Success Story" Society of Petroleum Engineers 2010.

20. Salavatov, T.S. and Ghareeb, A., "Predicting the behaviour of water and gas coning in horizontal wells", Oil and Gas Business 2009.

21. Brown, K.E., "Technology of Artificial Lift Methods", Penn Well Publishing Company, Tulsa, Oklahoma, 1984.

22. Bekbauov, B.E., et al., "Numerical modeling of the effects of disproportionate permeability reduction water-shutoff treatments on water coning", J. Energy Resour. Technol. 2013; 135(3): 011101–011110.

23. Howard, G.C. and Fast, C.R., "Squeeze Cementing Operations", AIME 1950; (189):53-64.

24. Smith, C.R. and Pirson, S.J., "Water Coning Control in Oil Wells by Fluid Injection". Society of Petroleum Engineers 1963.

25. Strickland, R.F., "Artificial barriers may control water coning", 1. Oil Gas J. 1974; (10):61–64.

26. Wojtanowicz, A.K., Hui, X., and Zaki, B., "Segregated production method for oil wells with active water coning", J. Pet. Sci. Eng. 1994; 11(1): 21–35.

27. Yue, P., et al., "The critical parameters of a horizontal well influenced by a semi-permeable barrier considering thickness in a bottom water reservoir", Journal of Petroleum Science and Engineering 2015; 129:88-96.

28. Yue, P., et al., "The critical rate of horizontal wells in bottom-water reservoirs with an impermeable barrier", Pet. Sci. 2012; 9(2): 223–228.

29. Jin, L. and A.K. Wojtanowicz A.K., "Analytical Assessment of Water-free Production in Oil Wells with Downhole Water Loop for Coning Control", SPE Production and operations symposium 2011.

30. Jin, L., A.K. Wojtanowicz, and R.G. Hughes, "An Analytical Model for Water Coning Control Installation in Reservoir with Bottom Water", Journal of Canadian Petroleum Technology 2010; 49(5): 65-70.

31. Yu, H., et al., "Case Study of Blocking Water Coning in Horizontal Well for Steam Stimulation in Heavy Oil Reservoir", SPE Asia Pacific Oil and Gas Conference and Exhibition 2016.

32. Temizel, C., et al., "Production Optimization under Injection of Biopolymer, Synthetic Polymer and Gels in a Heterogeneous Reservoir", SPE Eastern Regional Meeting 2016.

33. Ogienagbon, A., et al., "Experimental Investigation of the Feasibility of Polymer Flooding in a Shallow Niger Delta Oil Reservoir", SPE Nigeria Annual International Conference and Exhibition 2016.

34. Singhal, A.K., "Water And Gas Coning/Cresting - A Technology Overview", Petroleum Society of Canada 1993.

35. Singhal, A.K., "Water And Gas Coning/ Cresting A Technology Overview". Petroleum Society of Canada 1996.

36. Schevchenko, E., "Experimental study of water coning phenomenon in perforated pipes". 2013:1-77.

37. Smith, C., et al., "Case Study: Kazakhstan's First Application of Inflow Control Devices ICDs for Horizontal Wells", IADC/SPE Asia Pacific Drilling Technology Conference 2016.

38. Yue, P., et al., "The critical parameters of a horizontal well influenced by a semi-permeable barrier in bottom water reservoir", Petroleum Science, Springer 2015; (22):1448-1455.

39. Akangbou, H.N., Burby, M., and Ghasem, G., "Proactive control of cresting in homogeneous oil reservoirs - an experimental study", Petroleum Science 2017.